# Reliable Data Acquisition System for a Low-Cost Accelerograph Applied to Structural Health Monitoring

Milton Munoz[a], Remigio Guevara[b], Santiago Gonzalez[c*], Juan Carlos Jimenez[d]

[a]Red Sísmica del Austro, University of Cuenca, Av. 12 de Abril, Cuenca,010203, Ecuador
[b]Red Sísmica del Austro, University of Cuenca, Av. 12 de Abril, Cuenca,010203, Ecuador
[c]Department of Electric, Electronic and Telecommunication Engineering, University of Cuenca, Av. 12 de Abril, Cuenca,010203, Ecuador
[d]Red Sísmica del Austro, University of Cuenca, Av. 12 de Abril, Cuenca,010203, Ecuador

**Abstract**

This paper presents and evaluates a continuous recording system designed for a low-cost seismic station. The architecture has three main blocks. An accelerometer sensor based on MEMS technology (Microelectromechanical Systems), an SBC platform (Single Board Computer) with embedded Linux and a microcontroller device. In particular, the microcontroller represents the central component which operates as an intermediate agent to manage the communication between the accelerometer and the SBC block. This strategy allows the system for data acquisition in real time. On the other hand, the SBC platform is used for storing and processing data as well as in order to configure the remote communication with the station. This proposal is intended as a robust solution for structural health monitoring (i.e. in order to characterize the response of an infrastructure before, during and after a seismic event). The paper details the communication scheme between the system components, which has been minutely designed to ensure the samples are collected without information loss. Furthermore, for the experimental evaluation the station was located in the facilities on a relevant infrastructure, specifically a hydroelectric dam. The system operation was compared and verified with respect to a certified accelerograph station. Results prove that the continuous recording system operates successfully and allows for detecting seismic events according to requirements of structural health applications (i.e. detects events with a frequency of vibration less than 100 Hz). Specifically, through the system implemented it was possible to characterize the effect of a seismic event of 4 MD reported by the regional seismology network and with epicenter located about 30 Km of the hydroelectric dam. Particularly, the vibration frequencies detected on the infrastructure are in the range of 13 Hz and 29 Hz. Regarding the station performance, results from experiments reveals an average CPU load of 51%, consequently the processes configured on the SBC platform do not involve an overload. Finally, the average energy consumption of the station is close to 2.4 W, therefore autonomy provided by the backup system is aroud of 10 hours.

© 2021 Author(s).

*Keywords:* Data acquisition system, Internet of Things, real time processing, single board computer, structural health monitoring.

## 1. Introduction

The structural health monitoring represents a critical element for planning and development of urban areas characterized by resilience, sustainability and efficiency. Clearly, an appropriate and permanent evaluation performed on buildings, facilities and essential infrastructures (e.g. airports, ports, telecommunications towers, etc.), is the first

---

* Corresponding author.
*E-mail address*: santiago.gonzalezm@ucuenca.edu.ec (Santiago Gonzalez)

step toward the prevention and mitigation of disasters. It is worth mentioning that, the Structural Health is a multidisciplinary research field based on the cooperation of sciences such as, Civil Engineering, Seismology, Computer Science and even emerging technologies such the Internet of Things (IoT).

In regard to the events or conditions that are likely to cause damages on infrastructures, the seismic activity represents the most dramatic scenario to consider. In such a context, the role of the structural health monitoring consists in to characterize the buildings response before, during and after seismic events, i.e. detect some modifications of the fundamental vibration parameters (e.g. natural frequency, periods, mode shapes), methodology known as Operational Modal Analysis (OMA) [1], [2].

Based on the modal analysis, it is possible to identify those structural elements which have been affected and require intervention in order to mitigate potential risks. For example, in [3] and [4], the authors analyze the set-up of dampers and structural reinforcement elements on buildings, in order to reduce the effect of vibrations caused by earthquakes. In this context, it is worth highlighting that the seismic behavior along a specific zone can be induced or modified as result of human activities. In particular, activities such as groundwater extraction, fluid injection (e.g. artificial ponds), deployment of large underground networks for gas distribution or wastewater treatment, among others, are some of the factors that contribute to increasing the stress along geological faults and therefore the seismic risk on facilities and infrastructures [5].

With respect to natural events, seismic monitoring and prediction is an active research field. Although, it is not possible to determine exactly the location, magnitude and time for a next seismic event to occur in a region, there are substantial progress related to short-term earthquake prediction based on the analysis of seismic precursors. Specifically, there are some studies in the literature that describe a correlation between seismic events and indicators such as for example, anomalies in radon emission from soil [6], [7], weather fluctuations, fracto-emission peaks (i.e. acoustic, electromagnetic, and neutron emissions). In particular, the high frequency due to neutron emissions (scale of Tera Hertz), can be useful for detecting earthquakes in an initial phase as is described in [8] and [9]. Additional studies, also describe the possible relation between seismic events and electromagnetic anomalies detected in the ionosphere [10], [11], [12], thermal changes in the lithosphere [13], increasing of $CO_2$ in volcanic regions [14] and even, unusual behaviors in animals [15].

On the other hand, a promising and alternative research field consists in the analysis of microseismic events. This methodology involves the deployment of a large set of sensor nodes (i.e. accelerographs), with the aim of monitoring and characterizing the seismic behavior along a specific area or infrastructure. In this respect, transducers devices such as geophones and accelerometers are fundamental components for designing a continuous recording system. Even though, the cost of these sort of sensors is a factor to be consider, currently the application of MEMS technology (Microelectromechanical Systems) [16], particularly for accelerometers manufacturing, has contributed to a reduce both the costs and size of the stations and also has improved the sensors reliability. Regarding, structural health applications, it is appropriate to use MEMS accelerometers designed for low vibration frequencies (e.g. less than 100Hz) as is detailed in [17] and [18].

Furthermore, for designing a seismic station it is necessary to consider functionalities, as for example, data recording, data processing, network communication and remote management. With this end, it is possible to integrate the accelerometers along with reduced size computers also named Single Board Computers (SBC), such as Raspberry Pi, Odroid, Beaglebone, among others platforms [19]. In this respect, the implementation of a reliability data acquisition systems (i.e. data acquisition without information loss), represents the most critical challenge to be faced, especially, due to SBC platforms have not been designed for executing process in real time, as is discussed in [20] and [21]. This constraint results critical for structural health monitoring, where data from sensors (i.e. number of samples and timestamps), must be captured with high accuracy (microseconds deviations).

Following this objective, this paper presents the design and evaluation of an architecture for the reliable data acquisition in a low-cost accelerograph. The implementation performed involves emerging technologies such as, MEMS accelerometers and SBC platforms. This proposal represents a meaningful improvement of the previous work described in [22]. Especially, in order to face the challenge of acquisition and processing samples in real time, the architecture includes a microcontroller device which operates as an agent between the accelerometer sensor and the SBC platform.

Moreover, the timestamps of samples are generated by means of a GPS module or through an RTC device (Real Time Clock) for those cases when the signal acquisition from satellites is not feasible. Results from experiments show the

architecture designed ensures the data acquisition with high precision and avoiding information losses. The main contributions of this work with respect to similar proposals, consist in the thorough design of a robust solution for a continuos recording system which contemplates the use of emerging and low-cost technology. Also, it is worth highlighting  the moderate energy consumption as well as the facility to integrate this solution with new communications arquitectures (eg. Internet of Things).

The rest of the paper is organized as follow. In Section 2, relevant related work is presented. Section 3, describes the methodology and the components for the station implemented. The experimental evaluation and results are shown in Section 4. Finally, conclusions are discussed in Section 5.

## 2. Related Work

The development and deploying of seismic instrumentation for structural health monitoring involve the use of emerging technologies, such as IoT systems and communication architectures based on Wireless Sensors Networks (WSN). In this context, the characterization of building and facilities with regard to seismic events results fundamental in order to improve resilience and efficiency of urban areas. The following are some of the most relevant and representative studies in the literature.

Structural health applications are various, for instance in [23], the authors propose a system in order to detect seismic events generated from landslides and rock falls based on the temporal and frequency analysis of signals. The proposal includes a total of seven seismic stations which allows the system to detect events at several hundred meters from the epicenter. In [24] and [25], experimental studies which evaluate the impact of earthquakes on water and gas distribution networks are presented, respectively. In particular, the tests consist in artificial seismic events generated through explosives in order to determinate pipelines response in regard to join deformations, pipe strains and accelerations effects.

Moreover, preventive maintenance on strategic infrastructures (e.g. telecommunications and electricity towers), is another relevant application of structural health. For instance, monitoring the proper operation of wind turbines by means of a sensor network made up of accelerometers, as is described in [26] and [27]. Additionally, in [28] the authors point out the significance of an earthquake catalogue for those zones where essential infrastructures require be located.

In [29], is presented a study for evaluating the structural state of a bridge with more than 100 years old which is subjected to daily load due to passengers and heavy vehicles. It is worth noting that structural monitoring carried out on bridges has a strong interest. For instance, in [30], is proposed an ITS system (Intelligent Transportation System) where vehicular traffic is managed in real time taking in to account the load conditions on a bridge.

On the other hand, regarding buildings evaluation, in [31], is proposed a project for monitoring the Pier Luigi Nervi Exhibition Centre (Turin-Italy), affected by the seismicity of the region. In particular, the main goal consists in determining the proper location for sensors considering the complex building architecture. A similar study is described in [32], in this case with the aim to monitoring the Cardarelli Hospital building (Campobasso-Italy), both during operational conditions and after seismic events.

Regarding monitoring architectures, in [33], a framework in order to disseminate earthquake warning messages is proposed. Specifically, the seismic information is provided by accelerometer sensors available in users devices (e.g. smartphones), also the system includes a processing stage for evaluating seismic intensity. A similar proposal is described in [34], in this case, the seismic station includes a geophone sensor, while the data processing is performed by means of cloud computing services.

In [35], the implementation of a seismograph for detecting events in volcanic areas is presented. To this end, the prototype includes an electromagnetic, sensor as well as $CO_2$, temperature and pH sensors. In [36], the authors propose a seismic warning system through deployment of a wireless sensor network based on Zigbee technology. On the other hand, in regard to sensors reliability, in [17] a detailed analysis of the main seismic sensors for structural health applications, is presented. This study, highlight that seismic sensors based on MEMS technology result effective for data acquisition even under noise conditions and also provide the advantage of can be easily integrated along with wireless devices.

For instance, in [37], the authors present an experimental study carried out in the locality of Acireale (Sicilia-Italy)

where about of 100 seismic stations based on MEMS accelerometers were deployed. This sensor network aims at achieving a prompt evaluation of damages or potential risks caused by earthquakes. In [38] and [39], are presented additional studies where the application of MEMS accelerometers for structural health monitoring is emphasized.

In regard to data acquisition and processing, SBC platforms represent a proper alternative. In particular, the main advantages of SBC platforms are its low-cost, high performance, network communication capabilities, peripherals interfaces (e.g. SPI, I2C, UART), all integrated into a reduced-size electronic board. Moreover, the applications are various, for instance, home automation [40], smart access systems (e.g. access systems based on face recognition) [41], robotics applications [42], among others. However, it is significant consider that these sort of devices with embedded Linux, have not been designed for executing processes in real time which represents the major drawback of SBC platforms. This limitation results critic for systems where data acquisition must be performed with high accuracy, such as the seismic monitoring.

In order to address this issue, some studies and approaches in the literature suggest using Real Time Operating Systems (RTOS). Nevertheless, this strategy depends on the hardware used and also requires a deep knowledge about Linux systems. In this context, there are frameworks designed to reduce the complexity associated with using RTOS.

For instance, in [43] and [44], the authors propose the use of Xenomai [45], which consists in a framework that works along with the Linux Kernel for executing processes in real time. Finally, authors describe that although Xenomai contributes to reduce the latency, some limitations with respect to expected operation still persists. In this sense, an alternative solution consists in using intermediate devices (e.g. microcontrollers and processors) for data acquisition while the data processing and network communication functionalities are performed by means of the SBC platform.

The aforementioned alternative has been implemented in this work, specifically through of a microcontroller for data acquisition in real time.

Following, Section 3, presents the architecture proposed for the accelerograph station and the continuous recording system.

## 3. Methodology and Components

This section presents the proposed architecture for the accelerograph, especially the main components used as well as the solution designed for the data acquisition which ensures the capture of samples without loss of information. Finally, the software developed for the continuous recording system is described.

### 3.1. Accelerograph Component and Design

Fig. 1, depicts the architecture designed for the accelerograph. It can be seen that the central component consists in the microcontroller dsPIC33EP256MC [46], which has three main functions: reading samples from the accelerometer, generating a data frame including the sample number and timestamp and finally transmitting data to the SBC platform which consists in a Raspberry Pi 3 [47].

The aforementioned tasks have been defined due to the microcontroller (μC) is appropriate for executing processes in real time (i.e. sampling and digital signal processing).

On the other hand, the Raspberry Pi (RPi) due to it consists in a reduced-size computer with Linux embedded is most useful for managing files, storing data and configuring network communication.

Regarding the communication between the components, it was performed by means of a SPI bus (Serial Peripheral Interface). In particular, the μC operates as the master device in relation to the accelerometer while the RPi operates as the master device in relation to the μC. The main technical characteristics for the μC are detailed in Table 1.

Furthermore, the architecture includes the GPS module FGPMMOPA6H [48] and the RTC module DS3234 (Real Time Clock) [49]. These modules have been used with the purpose of generating the timestamps during the sampling process. In this context, the GPS provides the main signal by means of the PPS output (Pulse-per-second signal) while the RTC module provides a backup signal through the SWQ output. This backup signal is useful for those locations where the data acquisition from the satellites is not feasible.
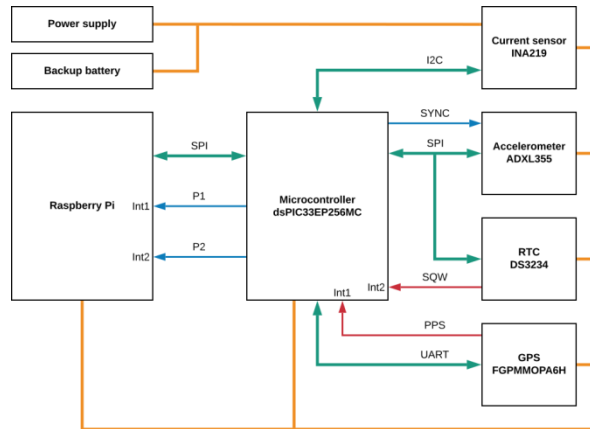
**Fig. 1** Accelerograph architecture and components

**Table 1.** Technical Specifications for the Microcontroller DSPic33EP256MC

| Parameter | Specification | Unit |
|---|---|---|
| Voltage operation | 3.0 to 3.6 | V |
| Operating temperature | -40 to +125 | ºC |
| Timer | Three 16-bit timers | Can pair up two to make one 32-bit |
| Analog features | ADC configurable module | 10 bits, 1.1 Msps, 12 bits, 500 ksps |
| UART | One module | 10 Mbps |
| SPI interfaces | Two modules | 15 Mbps |
| I2C interfaces | Two modules | 1 Mbaud |

It is worth highlighting that the timestamps are essentials for the proper operation of the accelerograph due to the fact that samples must be captured during specific time intervals. In this context, according to the technical specifications the accuracy achieved by means of the GPS module is 10 ns [48]. On the other hand, the RTC module has an accuracy of $\pm$ 2 ppm [49] or a variation equivalent of 2 μs by each second lapsed from the last synchronization event. Considering the aforementioned behavior, the data frame generated by the μC includes a field with the purpose to identify the samples captured when the GPS module is operative and the samples captured when the RTC module is active. This functionality is useful in order to carry out adjustments during the data processing.

Regarding the accelerometer, the design includes the ADXL355 MEMS sensor [50] characterized by a low noise density, an output resolution of 20 bits per channel (i.e. x, y and z axes) and low energy consumption.

**Table 2**. Technical Specifications for the MEMS Accelerometer ADXL355

| Parameter | Specification | Unit |
|---|---|---|
| Voltage operation | 2.25 to 3.6 | V |
| Operating temperature | - 40 a + 125 | ºC |
| Current demanded | 200 | μA |
| Measurement range | $\pm$ 2, $\pm$ 4, $\pm$ 8, $\pm$ 16 | g |
| Output resolution | 20 per channel | bits |
| Sensitivity at $\pm$ 2g | 256000 | LSB/g |
| Bandwidth | 1000 | Hz |
| Communication Interfaces | SPI/I2C | - |

Additionally, this sensor incorporates a set of internal registers which allow for storing samples, getting accelerometer status and setting operational parameters. For instance, the accelerometer includes a programmable high-and-low pass digital filters, therefore it is possible to configure the events detection considering structural health applications (i.e. events with a frequency of vibration less than 100 Hz). The main technical characteristics for the ADXL355 sensor

are detailed in Table 2.

Concerning data reading, it is necessary to take into account that the accelerometer provides the samples according to a configurable parameter named ODR (Output Data Rate). Additionally, the ODR value depend on the cut-off frequency configured for the internal low pass filter. In Table 3, the relationship between the ODR parameter and the cut-off frequency is detailed according to [50]. Therefore, considering the structural health field where the events analysis involves frequencies less than 100 Hz [17], [18], the cut-off frequency for the low pass filter was configured in 62.5 Hz which correspond to an ODR value of 250 (i.e. 250 samples per second). Moreover, in order to ensure that the samples match with the timestamps obtained from the GPS/RTC, it was necessary to configure an external synchronization mode on the accelerometer. That is, the μC provides to the accelerometer an external synchronization signal (sync signal) with the same frequency that the ODR value (i.e. 250 Hz or a sampling period of 4ms).

**Table 3.** Relationship between the ODR Value and the Low Pass Filter (LPF) Configuration

| Setting | ODR (Hz) | LPF (Hz) |
|---------|----------|----------|
| 0000 | 4000 | 1000 |
| 0001 | 2000 | 500 |
| 0010 | 1000 | 250 |
| 0011 | 500 | 125 |
| 0100 | 250 | 62.5 |
| 0101 | 125 | 31.25 |
| 0110 | 62.5 | 15.625 |
| 0111 | 31.25 | 7.813 |
| 1000 | 15.625 | 3.906 |
| 1001 | 7.813 | 1.953 |
| 1010 | 3.906 | 0.977 |

On the other hand, the ADXL355 accelerometer includes an internal FIFO buffer (first in, first out), which can be used for storing the samples in the same order as the information is generated. In particular, this buffer consists in a total of 96 memory positions (24 bits per position), which corresponding to 32 data sets with information of each channel (x, y, z, axes). Therefore, the reading process must be performed in a multi-byte mode in order to capture the information of each set of data. The frame structure is depicted in Fig. 2. As can be seen, it is necessary a total of 9 bytes in order to storing each data set in the μC.

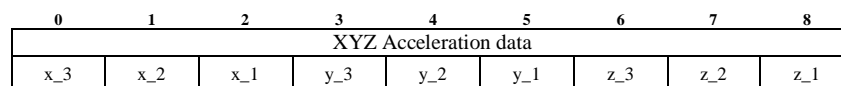| 0 | 1 | 2 | 3 | 4 | 5 | 6 | 7 | 8 |
|---|---|---|---|---|---|---|---|---|
| XYZ Acceleration data | | | | | | | | |
| x_3 | x_2 | x_1 | y_3 | y_2 | y_1 | z_3 | z_2 | z_1 |

Fig. 2 Frame structure for a data set with acceleration samples from x, y and z axes.

Concerning power supply, the accelerograph can be powered from the electricity grid or alternatively the architecture also contemplates a backup-battery of 24Wh. Additionally, the current sensor INA219 [51] was included in order to characterize the energy consumption demanded by the station. Following, in Section III-B, the communications process for data acquisition is detailed.

## 4. Experimental Evaluation

This section presents a set of experiments carried out with the aim to evaluate the accelerograph implemented (that has been named RSA station). Following this end, the RSA station was located along with a certified accelerograph in order to compare data collected. Furthermore, operational parameters (e.g. CPU load, temperature and energy consumptions), were monitored during the experiments for characterizing the station performance.

### 4.1. Structural Health Monitoring

In order to verify the proper operation of the RSA station for structural health applications, the accelerograph was installed on a relevant infrastructure. Specifically, the Chanlud hydroelectric dam, which is located to 25 Km from the

city of Cuenca in Ecuador (Lat -2.6753°, Long -79.0283°). In particular, this hydroelectric dam has a height of 60 m with a reservoir capacity of 17 million cubic meters of water [52]. The acceleration data collected by the RSA station were compared with the acceleration values detected by means of a reference equipment, particularly an ETNA model accelerograph developed by Kinemetrics. The ETNA technical specifications are detailed in [53] and [54]. Fig. 8, depicts the ubication of the Chanlud hydroelectric dam along with a photograph of the site. Additionally, the location of the accelerographs on the infrastructure is highlighted.

The acceleration data was collected during a period of three months. During this period some low-intensity seismic events were reported through the geophones network deployed in the region by the Research Department Red Sísmica del Austro of the University of Cuenca (Ecuador) [55]. However, an event detected on 26 march 2020 deserve special mention, due to the relative proximity with the site of the experiments. The epicenter was located about 30.32 Km to the north of the Chanlud, (Suscal locality highlighted on the map in Fig. 8) the event magnitude reported was of 4.0 Md and occurred at a depth of 13.36 Km. Following, results from both RSA station and the ETNA accelerograph are detailed.



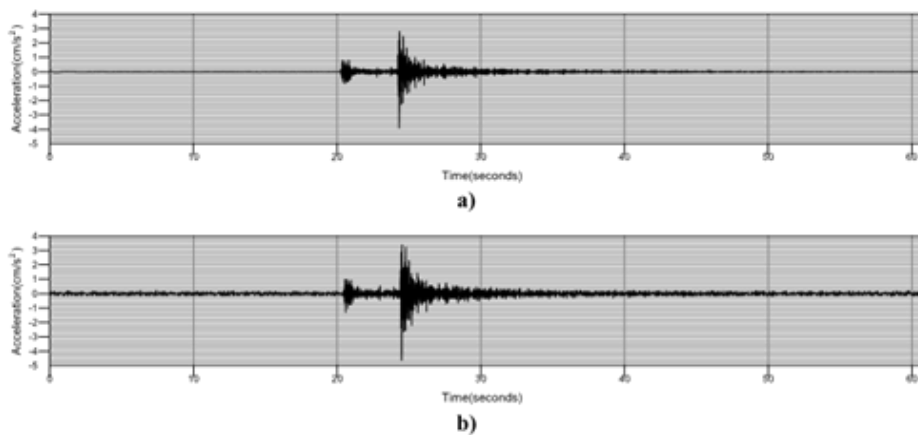Fig. 8  Ubication of the accelerographs on the Chanlud hydroelectric dam



Fig. 9  Accelerograms for the longitudinal component a) ETNA b) RSA station
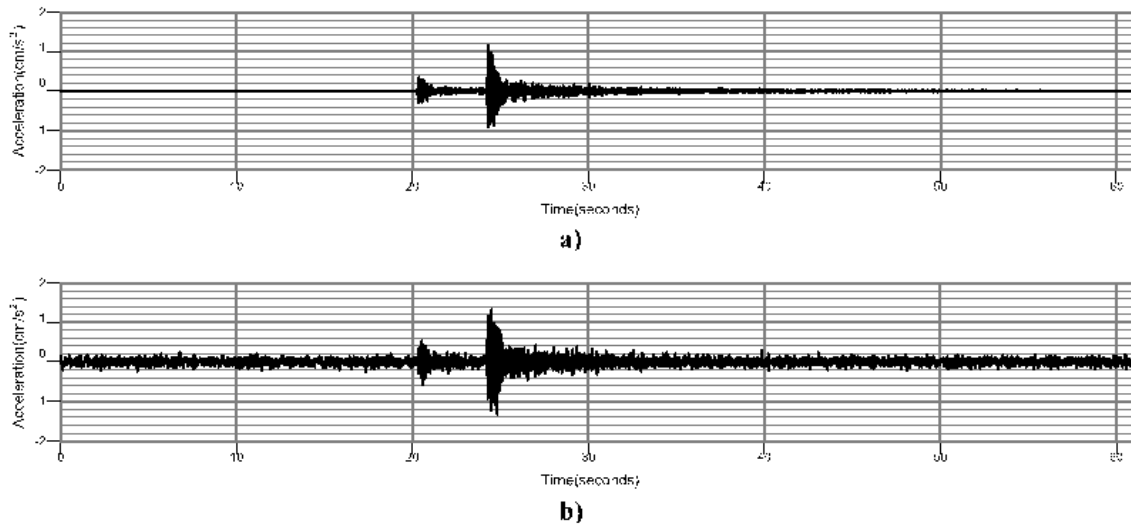
Fig. 10  Accelerograms for the transversal component a) ETNA b) RSA station

Fig. 9, Fig. 10 and Fig. 11, show, respectively, a comparison of the accelerograms corresponding to the longitudinal, transversal and the vertical component.  As can be observed, for each component the diagrams present a close similarity regarding both the amplitude values of acceleration and the shape of the signals obtained. Specifically, the amplitude difference between the maximum values of acceleration registered by the stations, were of 19.31% for the longitudinal axe and 15.24% in the case of the transversal axe.
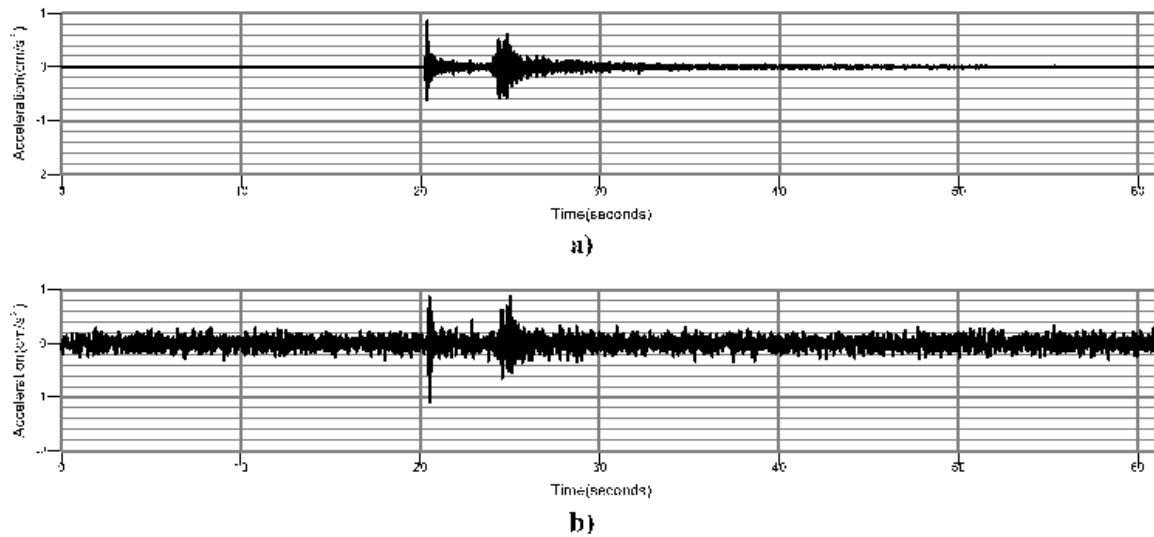


Fig. 11  Accelerograms for the vertical component a) ETNA b) RSA station

On the other hand, in the case of the vertical component depicted in Fig. 11, it can be noted that the accelerograms corresponding to the RSA station present an additional noise level compared with the signal from the reference equipment. In this sense, from the multiple tests carried out, it could be noted that this behavior is mainly due to two noise sources. In first place, the quantization noise of the accelerometer sensor, parameter that is detailed in the technical specifications [50]. Also, during the experiments, it could be verified the presence of environmental noise which is generated by the continuous water discharge in the base of the hydroelectric dam. Consequently, this effect can be clearly appreciated in the vertical accelerogram, where the noise level is significant.

Regarding, the analysis of the phase difference between the signals, Figure 12, shows an overlap for the case of the longitudinal components.  As can be appreciated, there is an accurate synchronization among the accelerograms,

behavior that evidences the proper operation of the RSA station.

Additionally, Fig. 13, Fig. 14 and Fig. 15, present, respectively, results regarding the comparison of the frequency spectrum for each component, i.e. longitudinal, transversal and vertical.

Particularly, Fig. 13, depicts the behavior for the longitudinal component where despite the amplitude differences, there is an exact match of the fundamental frequencies registered by the sensors (i.e. 16.9 Hz, 19.15 Hz and 25.9 Hz). Also, in this worth mentioning that in general, the longitudinal and transversal components are particularly significant when seismic analysis are performed on infrastructures, as is highlighted in several studies in the literature, as for example [56], [57] and [58]. With regard to amplitude variations, the differences can be attributed to the internal processing mechanisms carried out by the ETNA accelerograph which are detailed in [54], (e.g. antialiasing filters and frequency decimation).
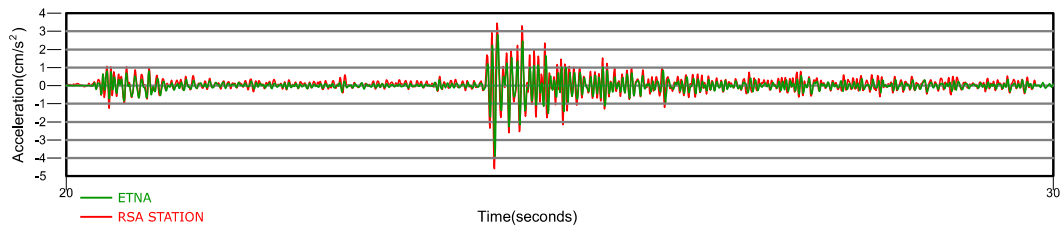

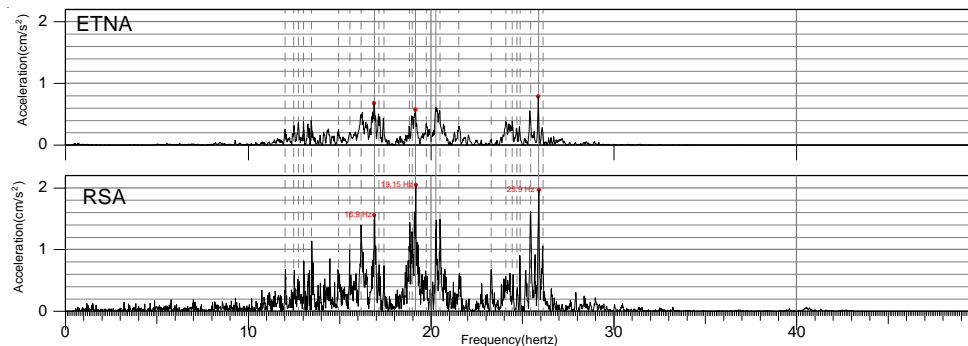Fig. 12 Phase difference analysis for the longitudinal component


Fig. 13 Comparison of the frequency spectrum for the longitudinal component

In that sense, it is worth clarifying that the raw data from the ETNA accelerograph is not available (i.e. the acceleration data provided by the analog sensor before the application of processing mechanisms). Therefore, the direct comparison of the acceleration values is restricted.

In the case of the transversal component depicted in Fig. 14, it can be observed the presence of additional frequencies on the spectrum of the RSA station. This effect is consequence of the noise components, as can be verified in the accelerogram of the Fig. 10. However, it is worth noting that the amplitude for the frequency values corresponding to the seismic event are more prominent that the noise components, as is detailed on the diagrams, i.e. for the frequency values of 13.45 Hz, 19.68 Hz and 29 Hz. Finally, in the case of the vertical component presented in Fig. 15, the noise sources previously analyzed (i.e. quantization noise and environmental noise) result in a significant distortion of the spectrum compared with results obtained by means of the ETNA accelerograph. Nevertheless, despite these differences, the comparison performed reveals the proper operation of the RSA station. In particular, it can be stated that the architecture implemented allows for the analysis and detection of local seismic events (i.e. for structural health applications) with a magnitude equal or higher than 4 Md. Following, in Section IV-B, results from the station performance are detailed.

## 4.2. Station Performance Evaluation

This section describes the results obtained regarding the station performance. In particular, system parameters such as the CPU load and temperature on the RPi platform as well as the energy consumption demanded by the station were evaluated. In this sense, it is worth highlighting the importance of verifying the operation of a continuous recording

system during long periods. Therefore, the information was collected at intervals of ten minutes during a period of a month. For this purpose, a monitoring software was developed in Python.
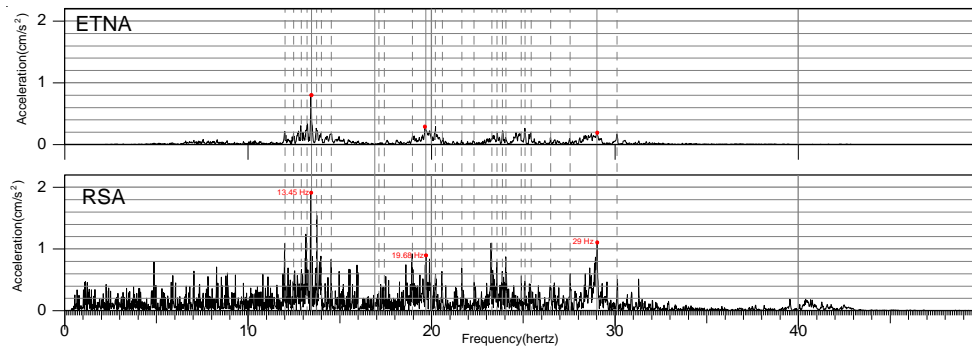


Fig. 14  Comparison of the frequency spectrum for the transversal component
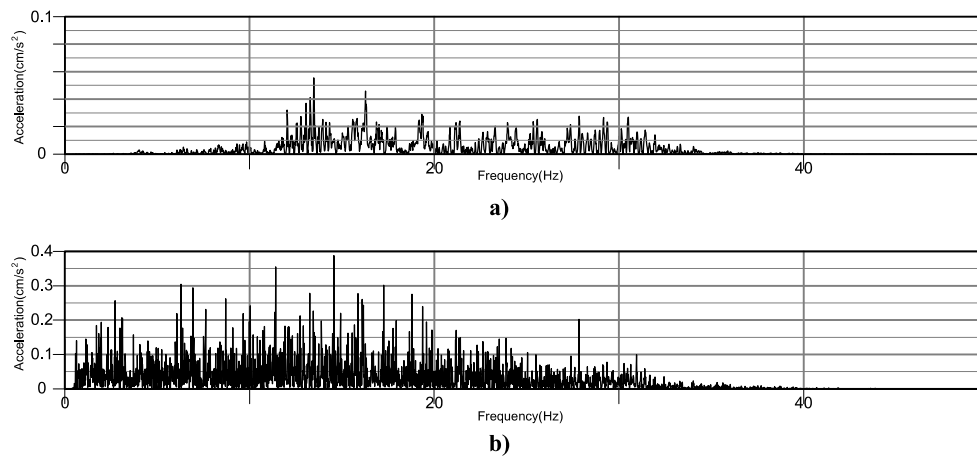


**a)**



**b)**

Fig. 15  Frequency spectrum for the vertical component a) ETNA b) RSA station

Fig. 16 depicts the behavior of the CPU load during a month of operation, where each sample on the graphic correspond to the average of the values measured per day. Results are presented with a 95% level of confidence. As can be seen, there are minimal changes on the CPU load, particularly the average value is close to 51%. Consequently, the processes required on the RPi platform (i.e. μC – RPi communication and the continuous recording system) do not involve an overload of the CPU.

Regarding the CPU temperature, results are shown in Fig. 17. It is worth indicating that usually the temperature value strongly depends on the CPU load. In that sense, despite the minimal changes detailed in Fig. 16, it can be observed that temperature value varies from 41ºC to 45ºC. This is due mainly to the changes in the ambient temperature detected along the experiment duration (one month). However, this behavior, the higher value registered for the CPU temperature was close to 46ºC which is distant from the maximum value recommended for a proper operation of the RPi platform (70ºC) as is described in technical specifications.

On the other hand, the energy consumption demanded by the station was evaluated by means of the INA219 sensor which allows for the capture of both samples of current and voltage, simultaneously. Fig. 18, shows the results regarding the power expenditure along the experiment duration. In particular, it is worth noting the narrow confidence intervals (95% confidence level) meaning minimal variation among samples, specifically within a range of between 2.37 W and 2.57 W. Additionally, the average consumption for the station is close to 2.4 W. Accordingly, taking into account the battery capacity included for the energy backup system (24 Wh), the station autonomy is close to 10 hours.
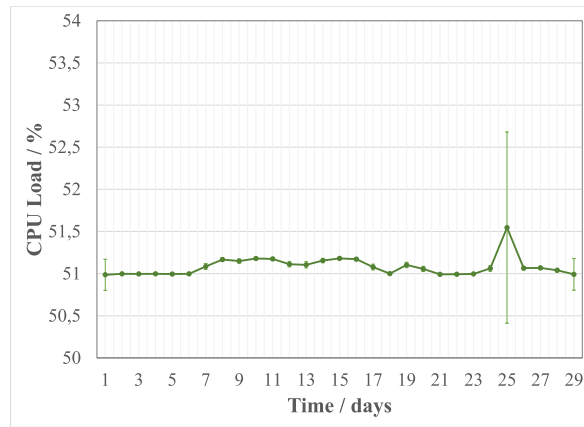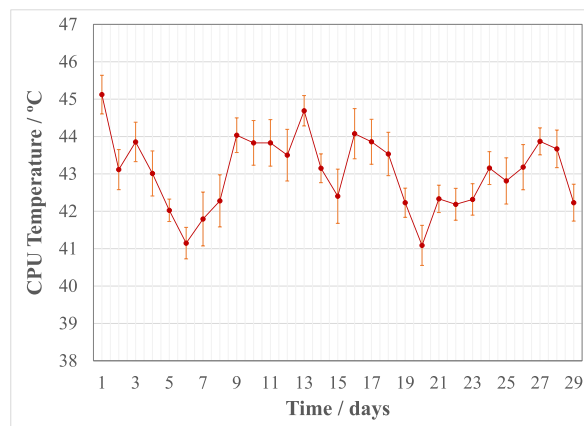
Fig. 16  CPU load monitoring
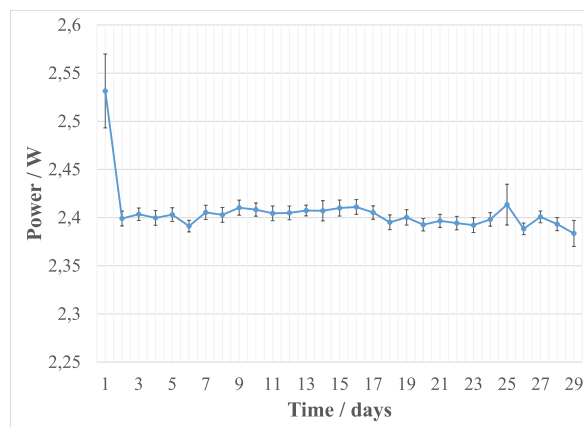


Fig. 17  CPU temperature monitoring



Fig. 18  Power samples captured during the prototype operation

## 5. Conclusion

In this paper, we presented the design and implementation of a continuous recording system for a low-cost accelerograph station. The solution proposed incorporates emerging technology. Particularly a MEMS accelerometer

as well as an SBC platform with embedded Linux. Additionally, a microcontroller device was included on the architecture, which operates as an intermediate agent in order to ensure both the reliable capture of samples and the execution of processes in real time. Moreover, for synchronization purposes the system includes a GPS module as well as RTC module as backup signal. Regarding the accelerometer it was configured for capturing a total of 250 samples per second. Also, the internal low-pass filter was set with a cutoff frequency of 62.5Hz, that represents a proper value considering the recommendations for structural health applications (i.e. frequencies of vibration less than 100 Hz).

With regard to the experimental evaluation the station was located in a relevant infrastructure (a hydroelectric dam) along with a certified equipment, for comparison purposes. Results collected from a seismic event which was reported by the regional seismology network, reveals that the acceleration values registered with the station are similar to the reference equipment. In particular, the differences obtained regarding the maximum acceleration values were 19% and 15% for the longitudinal and transversal components, respectively. Furthermore, results describe an exact match with regard both the phase and the frequency spectrum of the signals. Specifically, in the case of the longitudinal component the fundamental vibration frequencies caused by the seismic event on the infrastructure, were of 16.9 Hz, 19.15 Hz and 25.9 Hz. In the case of the transversal components the frequencies registered were of 13.45 Hz, 19.68 Hz and 29 Hz. In this context, it is worth highlighting, that the longitudinal and transversal components are particularly significant for evaluating the impact of a seismic event on an infrastructure.

On the other hand, in the case of the vertical component, results present a notable difference between the spectrum diagrams. However, from the multiples experiments it could be verified that these differences are caused by noise sources, particularly due to the continuous water discharge in the base of the hydroelectric dam. Finally, a set of experiments were carried out in order to evaluate the station performance. In particular, an average CPU load of 51% was detected during the system operation. Therefore, the processes configured do not involve an overload of the CPU.

Additionally, with regard to the CPU temperature the maximum value obtained, was close to 46ºC, that is, distant from the peak value described in the technical specifications of the RPi platform. Finally, the energy autonomy when the RSA station operates with the backup power system (i.e. battery) is close to 10 hours. Consequently, results show the proper operation of the station implemented that represents the main contribution of this work to the design of solutions used in applications of structural health.

## Acknowledgements

## References

[1]     G. Lacanna, M. Ripepe, M. Coli, R. Genco, and E. Marchetti, "Full structural dynamic response from ambient vibration of Giotto's bell tower in Firenze (Italy), using modal analysis and seismic interferometry," *NDT E Int.*, vol. 102, no. November 2018, pp. 9–15, 2019.

[2]     A. Bayraktar, T. Türker, and A. C. Altunişik, "Experimental frequencies and damping ratios for historical masonry arch bridges," *Constr. Build. Mater.*, vol. 75, pp. 234–241, 2015.

[3]     J. He, Y. L. Xu, S. Zhan, and Q. Huang, "Structural control and health monitoring of building structures with unknown ground excitations: Experimental investigation," *J. Sound Vib.*, vol. 390, pp. 23–38, 2017.

[4]     S. Hou, C. Zeng, H. Zhang, and J. Ou, "Monitoring interstory drift in buildings under seismic loading using MEMS inclinometers," *Constr. Build. Mater.*, vol. 185, pp. 453–467, 2018.

[5]     C. Doglioni, "A classification of induced seismicity," *Geosci. Front.*, vol. 9, no. 6, pp. 1903–1909, 2018.

[6]     A. Deb, M. Gazi, J. Ghosh, S. Chowdhury, and C. Barman, "Monitoring of soil radon by SSNTD in Eastern India in search of possible earthquake precursor," *J. Environ. Radioact.*, vol. 184–185, no. January, pp. 63–70, 2018.

[7]     A. D. K. Tareen, M. S. A. Nadeem, K. J. Kearfott, K. Abbas, M. A. Khawaja, and M. Rafique, "Descriptive analysis and earthquake prediction using boxplot interpretation of soil radon time series data," *Appl. Radiat. Isot.*, vol. 154, no. July, 2019.

[8]     A. Carpinteri and O. Borla, "Fracto-emissions as seismic precursors," *Eng. Fract. Mech.*, vol. 177, pp. 239–250, 2017.

[9]     A. Carpinteri and O. Borla, "Acoustic, electromagnetic, and neutron emissions as seismic precursors: The lunar periodicity of low-magnitude seismic swarms," *Eng. Fract. Mech.*, vol. 210, no. April 2018, pp. 29–41, 2019.

[10]    K. I. Oyama *et al.*, "Precursor effect of March 11, 2011 off the coast of Tohoku earthquake on high and low latitude ionospheres and its possible disturbing mechanism," *Adv. Sp. Res.*, vol. 63, no. 8, pp. 2623–2637, 2019.

[11]    A. Mahmoudian and M. J. Kalaee, "Study of ULF-VLF wave propagation in the near-Earth environment for earthquake prediction," *Adv. Sp. Res.*, vol. 63, no. 12, pp. 4015–4024, 2019.

[12]    C. Sotomayor-Beltran, "Ionospheric anomalies preceding the low-latitude earthquake that occurred on April 16, 2016 in Ecuador," *J. Atmos. Solar-Terrestrial Phys.*, vol. 182, no. October 2018, pp. 61–66, 2019.

[13]    M. Khalili, S. K. Alavi Panah, and S. S. Abdollahi Eskandar, "Using Robust Satellite Technique (RST) to determine thermal anomalies before a strong earthquake: A case study of the Saravan earthquake (April 16th, 2013, M W = 7.8, Iran)," *J. Asian Earth Sci.*, vol. 173, no. January, pp. 70–78, 2019.

[14]    L. Pierotti, F. Gherardi, G. Facca, L. Piccardi, and G. Moratti, "Detecting CO2 anomalies in a spring on Mt. Amiata volcano (Italy)," *Phys. Chem. Earth*, vol. 98, pp. 161–172, 2017.

[15]    R. A. Grant and T. Halliday, "Predicting the unpredictable; evidence of pre-seismic anticipatory behaviour in the common toad," *J. Zool.*, vol. 281, no. 4, pp. 263–271, 2010.

[16]    G. Langfelder and A. Tocchio, *Microelectromechanical systems integrating motion and displacement sensors*. Elsevier Ltd, 2018.

[17]    S. Das and P. Saha, "A review of some advanced sensors used for health diagnosis of civil engineering structures," *Meas. J. Int. Meas. Confed.*, vol. 129, no. January, pp. 68–90, 2018.

[18]    P. Pachón, R. Castro, E. García-Macías, V. Compan, and E. Puertas, "E. Torroja's bridge: Tailored experimental setup for SHM of a historical bridge with a reduced number of sensors," *Eng. Struct.*, vol. 162, no. September 2017, pp. 11–21, 2018.

[19]    U. Isikdag, "Internet of Things: Single-Board Computers," in *Enhanced Building Information Models: Using IoT Services and Integration Patterns*, Springer International Publishing, 2015, pp. 43–53.

[20]    D. Molloy, "Interfacing to the Raspberry Pi Buses," in *Exploring Raspberry Pi Interfacing to the Real World with Embedded Linux*, Wiley, 2016, pp. 219–274.

[21]    F. Reghenzani, G. Massari, and W. Fornaciari, "The real-time linux kernel: A survey on Preempt_RT," *ACM Comput. Surv.*, vol. 52, no. 1, 2019.

[22]    S. González, J. C. Jiménez, R. Guevara, and I. Palacios, "IoT-based Microseismic Monitoring System for the Evaluation of Structural Health in Smart Cities," in *Congreso Iberoamericamo de Ciudades Inteligentes (ICSC-CITIES), Soria, Valladolid-Spain*, 2018, pp. 191–203.

[23]    V. L. Zimmer and N. Sitar, "Detection and location of rock falls using seismic and infrasound sensors," *Eng. Geol.*, vol. 193, pp. 49–60, 2015.

[24]    C. Wang, W. Liu, and J. Li, "Artificial earthquake test of buried water distribution network," *Soil Dyn. Earthq. Eng.*, vol. 79, pp. 171–185, 2015.

[25]    H. Miao, W. Liu, C. Wang, and J. Li, "Artificial earthquake test of gas supply networks," *Soil Dyn. Earthq. Eng.*, vol. 90, no. February, pp. 510–520, 2016.

[26]    Z. Herrasti, I. Val, I. Gabilondo, J. Berganzo, A. Arriola, and F. Martínez, "Wireless sensor nodes for generic signal conditioning: Application to Structural Health Monitoring of wind turbines," *Sensors Actuators, A Phys.*, vol. 247, pp. 604–613, 2016.

[27]    G. Kilic and M. S. Unluturk, "Testing of wind turbine towers using wireless sensor network and accelerometer," *Renew. Energy*, vol. 75, pp. 318–325, 2015.

[28]    K. Dai, K. Gao, and Z. Huang, *Environmental and Structural Safety Issues Related to Wind Energy*. Elsevier Inc., 2017.

[29]    E. Ghafoori, A. Hosseini, R. Al-Mahaidi, X. L. Zhao, and M. Motavalli, "Prestressed CFRP-strengthening and long-term wireless monitoring of an old roadway metallic bridge," *Eng. Struct.*, vol. 176, no. June, pp. 585–605, 2018.

[30]    H. Malik and W. Zatar, "Software Agents to Support Structural Health Monitoring (SHM)-Informed Intelligent Transportation System (ITS) for Bridge Condition Assessment," *Procedia Comput. Sci.*, vol. 130, pp. 675–682, 2018.

[31]    E. Lenticchia, R. Ceravolo, and C. Chiorino, "Damage scenario-driven strategies for the seismic monitoring of XX century spatial structures with application to Pier Luigi Nervi's Turin Exhibition Centre," *Eng. Struct.*, vol. 137, pp. 256–267, 2017.

[32]    D. Gargaro, C. Rainieri, and G. Fabbrocino, "Structural and seismic monitoring of the 'cardarelli' Hospital in Campobasso," *Procedia Eng.*, vol. 199, pp. 936–941, 2017.

[33]    A. M. Zambrano, I. Perez, C. Palau, and M. Esteve, "Technologies of Internet of Things applied to an Earthquake Early Warning System," *Futur. Gener. Comput. Syst.*, vol. 75, no. 2017, pp. 206–215, 2017.

[34]    M. Klapez, C. A. Grazia, S. Zennaro, M. Cozzani, and M. Casoni, "First Experiences with Earthcloud, a Low-Cost, Cloud-Based IoT Seismic Alert System," *Int. Conf. Wirel. Mob. Comput. Netw. Commun.*, vol. 2018-Octob, pp. 262–269, 2018.

[35]    N. Carreras, D. Moure, S. Gomáriz, D. Mihai, A. Mànuel, and R. Ortiz, "Design of a smart and wireless seismometer for volcanology monitoring," *Meas. J. Int. Meas. Confed.*, vol. 97, pp. 174–185, 2017.

[36]    A. Alphonsa and G. Ravi, "Earthquake early warning system by IOT using Wireless sensor networks," *Proc. 2016 IEEE*

*Int. Conf. Wirel. Commun. Signal Process. Networking, WiSPNET 2016*, pp. 1201–1205, 2016.

[37] A. D'alessandro *et al.*, "Monitoring Earthquake through MEMS Sensors (MEMS project) in the town of Acireale (Italy)," *5th IEEE Int. Symp. Inert. Sensors Syst. Inert. 2018 - Proc.*, pp. 1–4, 2018.

[38] S. Valenti *et al.*, "A low cost wireless sensor node for building monitoring," *EESMS 2018 - Environ. Energy, Struct. Monit. Syst. Proc.*, pp. 1–6, 2018.

[39] S. Sindhuja and J. S. J. Kevildon, "MEMS-based wireless sensors network system for post-seismic tremor harm evaluation and building monitoring," *IEEE Int. Conf. Circuit, Power Comput. Technol. ICCPCT 2015*, pp. 1–4, 2015.

[40] V. Vujović and M. Maksimović, "Raspberry Pi as a Sensor Web node for home automation," *Comput. Electr. Eng.*, vol. 44, pp. 153–171, 2015.

[41] M. Sajjad, M. Nasir, F. U. M. Ullah, K. Muhammad, A. K. Sangaiah, and S. W. Baik, "Raspberry Pi assisted facial expression recognition framework for smart security in law-enforcement services," *Inf. Sci. (Ny).*, vol. 479, pp. 416–431, 2019.

[42] S. E. Oltean, "Mobile Robot Platform with Arduino Uno and Raspberry Pi for Autonomous Navigation," *Procedia Manuf.*, vol. 32, pp. 572–577, 2019.

[43] R. Delgado, B. J. You, and B. W. Choi, "Real-time control architecture based on Xenomai using ROS packages for a service robot," *J. Syst. Softw.*, vol. 151, pp. 8–19, 2019.

[44] G. Johansson, "Real-Time Linux Testbench on Raspberry Pi 3 using Xenomai," KTH ROYAL INSTITUTE OF TECHNOLOGY, 2018.

[45] Xenomai.org, "Xenomai." .

[46] Microchip, "Data sheet dsPIC33EP256MC," Microchip, Available: https://www.microchip.com/design-centers/16-bit/products/dspic33e, [Accessed: 02-Dec-2019].

[47] RaspberryPi.org, "Raspberry Pi 3 Model B+," RaspberryPi.org, Available: https://static.raspberrypi.org/files/product-briefs/Raspberry-Pi-Model-Bplus-Product-Brief.pdf, [Accessed: 02-Dec-2019].

[48] GlobalTop Technology, "FGPMMOPA6H GPS Standalone Module Data Sheet," GlobalTop Technology, Available: https://cdn-shop.adafruit.com/datasheets/GlobalTop-FGPMMOPA6H-Datasheet-V0A.pdf, [Accessed: 02-Dec-2019].

[49] D. Semiconductor, "Extremely Accurate SPI Bus RTC with Integrated Crystal and SRA." Dallas Semiconductor, Available: https://www.sparkfun.com/datasheets/BreakoutBoards/DS3234.pdf, [Accessed: 02-Dec-2019].

[50] Analog Devices, "Low Noise, Low Drift, Low Power, 3-Axis MEMS Accelerometer ADXL355." Analog Devices, Available: https://www.analog.com/media/en/technical-documentation/data-sheets/adxl354_355.pdf, [Accessed: 02-Dec-2019].

[51] Adafruit Industries, "Technical specifications INA219 Current sensor." Adafruit Industries, Available: https://cdn-learn.adafruit.com/downloads/pdf/adafruit-ina219-current-sensor-breakout.pdf, [Accessed: 10-Jan-2020].

[52] ElecAustro, "Represa Chanlud." .

[53] Kinemetrics, "Technical specifications ETNA accelerograph." Available: http://cnrrs.utcb.ro/cnrrs_en/divizii/divizia2/doc/etna.pdf, [Accessed: 17-Jan-2020].

[54] Kinemetrics, "User Guide Etna Digital Recorder, Document 302230." https://docplayer.net/63635428-User-guide-etna-digital-recorder.html, [Accessed: 17-Jan-2020].

[55] Red Sísmica del Austro, "Reportes Red Sismica del Austro- Universidad de Cuenca -Ecuador." .

[56] X. Liang and K. M. Mosalam, "Ground motion selection and modification evaluation for highway bridges subjected to Bi-directional horizontal excitation," *Soil Dyn. Earthq. Eng.*, vol. 130, no. December 2019, p. 105994, 2020.

[57] S. M. Sah, J. J. Thomsen, and D. Tcherniak, "Transverse vibrations induced by longitudinal excitation in beams with geometrical and loading imperfections," *J. Sound Vib.*, vol. 444, pp. 152–160, 2019.

[58] J. Jiménez-Pacheco, R. González-Drigo, L. G. Pujades Beneit, A. H. Barbat, and J. Calderón-Brito, "Traditional High-rise Unreinforced Masonry Buildings: Modeling and Influence of Floor System Stiffening on Their Overall Seismic Response," *Int. J. Archit. Herit.*, vol. 00, no. 00, pp. 1–38, 2020.